Chapter 5

Supercapacitors: A Potential Application of Silica-Gel Solid Electrolytes for Energy Storage Devices

5.1 Introduction*

Rapid stride in different industrial areas, coupled with population hike has resulted in an ever-increasing demand for energy, which causes a major strain on the existing tools and techniques available for power production and energy-storage devices. Consequently alternative and efficient energy-storage devices and resources are being developed and explored. Supercapacitors are also known as electrochemical capacitors or as ultra-capacitors and are one of such kind known for their efficient energy storage and applications. These devices exhibit unique characteristics and variedly used from simple applications in electronics (conventional capacitors) to high voltage applications (supercapacitors). Since there is a lot of potential in the advancement of energy-storage device technologies, expertise in these devices has experienced tremendous growth [1]. We also find reports that mention the improvement of energy capacity of aqueous supercapacitors by engineering strategies [2]. In this chapter, we report the capacitance studies of some novel non-polymer based solid electrolytes mentioned in chapter 4.

5.1.1 Supercapacitor Type

In a detailed review Zhong *et al.* [3] have classified the electrochemical supercapacitors (ultra capacitors) into three categories viz; i) Electrochemical Double-Layer Capacitors (EDLCs), ii) pseudo capacitors and iii) hybrid-capacitors. Both pseudo capacitors and hybrid-capacitors involve faradaic redox reactions; in the present study the electrolyte materials developed mostly do not give rise to faradaic redox reactions and hence these systems are designated as EDLCs. In a few cases we may have to invoke redox reactions (which produce negligible faradaic activity) such as the case when we introduce heavy metal ions (Pb^{2+}) in the system, or the cationic part of the IL undergoes redox process etc. However, these cases are a few in numbers and hence we may classify the capacitors discussed in this chapter in general as EDLCs.

** Part of this work is published in (i) Materials Research Express, 6 (2019) 105202 and (ii) Electrochimica Acta, 323 (2019) 134841.*

The most accepted model of electrode- electrolyte environment is 'Electrical Double Layer' model given by Stern, which combines Helmholtz-Perrin and Gouy-Chapman models; this theory states that counter ions pack closely in the layer close to the electrode (known as a 'compact layer' and extends up to outer Helmholtz plane) and in subsequent electrolyte layers (known as 'diffused layer'), the concentration of ions and the potential decays. Based on this model one can calculate the "intrinsic capacitance". The "apparent capacitance" can be estimated from experiments such as impedance spectroscopy [4-5].

5.2 Experimental Procedures

5.2.1 Preparation of Electrode Material and Fabrication of Supercapacitor

Electrode material (activated carbon electrode) was prepared starting from coconut shells. Coconut shell was first converted to activated charcoal as per the following steps. The shell was ground completely to get a fine powder. This shell powder was then mixed with KOH (used as an activator) thoroughly. This mixture was then heated in a tube furnace at 800 ^{o}C for approximately 3 - 4 hours under constant nitrogen flow. The obtained charcoal was first neutralized using 0.1M HCl solution followed by thorough washing with deionised water. Later, it was dried at ~100 ^{o}C and stored in desiccator (Fig 5.1). In literature we find many such similar procedures [6].

The surface area of the activated charcoal used was found by BET method. Activated charcoal was then made into a paste for making the electrode. The electrode paste was prepared by a thorough mixing of activated charcoal (80%), acetylene black (10%), and PVDF (10%) with acetone as medium.

Fig. 5.1 Preparation procedure for cathode material (a) Coconut shells, (b) Cathode preparation-cleaning process after cathode formation, (c) activated Charcoal (surface area 260 m^2/g).

To measure the capacitance of the solid electrolytes (silica gel composites prepared as mentioned in Chapter 4), pellets of the same were made. Initially, the obtained samples

were mechanically ground into very fine powder and pellets were prepared under pressure (holder diameter 9 mm; 5 - 6 ton load for high Li containing composites and 1 - 2 ton load for high IL containing composites).

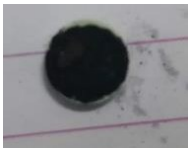

Fig. 5.2 Pellet obtained after applying the cathode paste.

The activated charcoal electrode thus prepared attached on both sides of the pellet (actually the paste was applied, dried, weighed) before fabrication of the supercapacitor cells (Fig. 5.2). These pellets were crimped into the cells prior to measurements (Fig. 5.3).

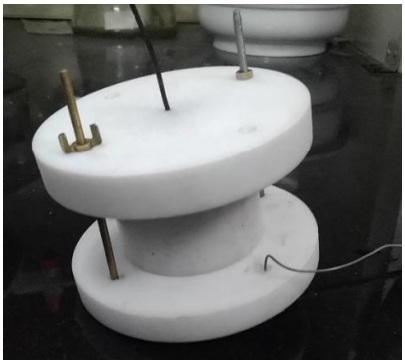

Fig. 5.3 Unit used for capacitance measurement.

Individual components of the supercapacitors are aligned carefully [7]. Supercapacitor cells can be designed in the form of a coin cell design, cylindrical cell design, and pouch cell design. In the present studies, the coin cell design was preferred for determining the capacitance of the electrolyte materials. The electrode material and its pore size, surface area etc. has been fixed and specific capacitance for various EDLCs have been calculated and tabulated.

5.2.2. Two Electrode Cell Configuration

Cyclic voltammetry is generally performed in three-electrode cell configuration, especially for liquid electrolyte based supercapacitors. It informs about the nature of the charge stored at individual interfaces of cathodic and anodic regions. However, for solid-state supercapacitors, the cyclic voltammetry is performed in two electrode cell configuration

where the overall behavior of the capacitor cell can be characterized. In the present work, the electrochemical behavior of the composites has been determined in two-electrode cell configuration (Electrode | Composite | Electrode) by cyclic voltammetry [8-9].

5.2.3 Calculation for Capacitance Values

Impedance spectroscopy and cyclic voltammetry were used to characterize the capacitance properties of the silica gel composites as reported in literature [9-10]. The impedance measurements were carried out using the LCR meter mentioned in chapter 2, in the frequency range from 1 mHz to 100 kHz. The overall capacitance value from impedance can be determined by using $C = 1/\omega Z''$, where ω is the angular frequency and Z'' is the imaginary part of the total complex impedance Z.

For the present work, the capacitance values of the composites were evaluated using C = i/s relation, where *i* is the current and s is the scan rate ($\Delta V/\Delta t$) in a cyclic voltammetry (CV) experiment. The capacitance of single electrode was further evaluated by multiplying the overall cell capacitance by a factor of 2 and dividing by the mass of the single electrode material. Scan rate of 10 mV/s was used for most of the measurements. For high temperature measurements the same arrangement that was set up for temperature variation in conductivity measurements is used.

5.3 Exploring applications of IL confined silica gels as Supercapacitors: Preliminary findings

In the following sections the capacitance studies of different IL confined silica gel composites are described. Some of the samples were prepared by two different procedures (hydrolytic and non-hydrolytic processes). We call these as preliminary findings for the following reasons (i) the electrode material's composition, activated charcoal's surface area are not optimized for best capacitance measurements; (ii) the sample particle size before pellet making and the pressure used for pellet making are not optimized; (iii) the sample composition (essentially the variation in Li and IL concentrations) was not optimized for the best capacitance; (iv) and we have not performed any galvanostatic charge/discharge studies and hence reliable estimations of charge densities and power densities could not be done and are not reported. These studies could not be completed due to time constraints and are suggested for future scope of this work. In Table 5.1 we list all

the composites and the capacitance value wherever it is measurable. The samples have been grouped according to the IL used and the method of preparation (hydrolytic/non hydrolytic). Only variable components mol % value is given (full details are available in Chapter 4). When the capacitance value is too low, the value of the capacitance is not shown in the corresponding column.

Table 5.1-Measured capacitance and other relevant information for the composites prepared in this work.

(indicates the sample entry is repeated for comparison with other entries in the group)*

S. No.	Sample Code	Li	IL	K	Conductivity at 305 K	Capacitance at 305 K
		(mol%)			(Ω^{-1} cm^{-1})	(Fg^{-1})
System 4A: [EMIM] BF_4 containing composites (Hydrolytic Process) Section 5.3.1.1						
Series-1						
1	L18	18	0	0	1.9×10^{-8}	**0.01**
2	L18E	18	1	0	2.3×10^{-7}	**0.1**
3	L26E	26	1	0	1.0×10^{-5}	**2.9**
4	L33E	33	1	0	1.5×10^{-4}	**6.5**
5	L40E	40	1	0	2.0×10^{-4}	**6.5**
6	L46E	46	1	0	6.5×10^{-5}	**10.9**
Series-2						
2*	L18E	18	1	0	2.3×10^{-7}	**0.1**
7	L18E2	18	2	0	9.9×10^{-8}	**0.01**
8	L18E4	18	4	0	2.9×10^{-9}	**0.03**
9	L18E7	18	7	0	2.6×10^{-10}	**-**
Series-3						
4*	L33E	33	1	0	1.5×10^{-4}	**6.5**
10	L33E2	33	2	0	5.3×10^{-5}	**-**
11	L33E3	33	3	0	3.9×10^{-8}	**1.3**
12	L33E7	33	7	0	2.3×10^{-9}	**-**
Series-4						
13	E4	0	4	0	2.8×10^{-10}	**-**
14	E8	0	8	0	2.1×10^{-9}	**-**
System 4B: [EMIM] BF_4 containing composites (Hydrolytic Process – KNO_3 substitution) Section 5.3.1.2						
Series-1						
15	L9K9	9	0	9	1.1×10^{-7}	**0.12**
16	L9K9E	9	1	9	2.9×10^{-6}	**0.02**
17	L16K16E	16	1	16	2.0×10^{-7}	**0.17**
18	L23K23E	23	1	23	1.5×10^{-6}	**0.05**
Series-2						
16*	L9K9E	9	1	9	2.9×10^{-6}	**0.02**
19	L9K17E	9	1	17	1.7×10^{-7}	**0.41**
20	L8K25E	8	1	25	3.4×10^{-6}	**0.07**

S. No.	Sample Code	Li	IL	K	Conductivity at 305 K	Capacitance at 305 K
		(mol%)			(Ω^{-1} cm^{-1})	(Fg^{-1})
Series-3						
21	L0K18	0	0	18	4.2×10^{-7}	-
22	L0K18E	0	1	18	1.7×10^{-6}	**0.01**
System 4C: [EMIM] BF_4 containing composites (Non-Hydrolytic Process) Section 5.3.1.3						
Series-1						
23	L18n	18	0	0	1.3×10^{-8}	-
24	L18En	18	1	0	3.2×10^{-7}	**0.12**
25	L26En	26	1	0	1.4×10^{-6}	**0.04**
26	L33En	33	1	0	1.0×10^{-6}	**0.04**
27	L40En	40	1	0	4.6×10^{-7}	**0.12**
28	L46En	46	1	0	8.9×10^{-7}	**0.46**
Series-2						
24*	L18En	18	1	0	3.2×10^{-7}	**0.12**
29	L18E2n	18	2	0	1.3×10^{-8}	**0.12**
30	L18E3n	18	3	0	7.7×10^{-9}	**0.09**
31	L18E7n	18	7	0	8.8×10^{-11}	-
Series-3						
30*	L18E3n	18	3	0	7.7×10^{-9}	**0.09**
32	L33E3n	33	3	0	3.8×10^{-6}	**0.71**
33	L40E3n	40	3	0	9.3×10^{-7}	**0.02**
34	L46E3n	46	3	0	7.6×10^{-8}	**0.52**
System 4D: [BMIM] Br containing composites (Hydrolytic Process) Section 5.3.2						
Series-1						
35	L10	10	0	0	8.5×10^{-9}	-
36	L10B	10	1	0	8.5×10^{-9}	-
37	L20B	20	1	0	5.8×10^{-5}	**7.6**
38	L25B	25	1	0	5.8×10^{-8}	**10.8**
39	L30B	30	1	0	1.4×10^{-7}	**14.1**
Series-2						
36*	L10B	10	1	0	8.5×10^{-9}	-
40	L10B2	10	2	0	1.9×10^{-5}	-
41	L10B4	10	4	0	4.7×10^{-10}	**0.5**
Series-3						
42	L10P	10	0	0	4.5×10^{-6}	-
43	L10PB	10	1	0	1.3×10^{-5}	-
44	L20PB	20	1	0	5.9×10^{-5}	**1.8**
45	L25PB	25	1	0	2.1×10^{-4}	**1.2**
System 4E: [EMIM] CF_3SO_3 containing composites (Hydrolytic Process)Section 5.3.3						
Series-1						
46	L18F	18	1	0	8.2×10^{-11}	-
47	L33F	33	1	0	6.2×10^{-6}	**11.4**
48	L46F	46	1	0	4.9×10^{-4}	**28**
Series-2						
46*	L18F	18	1	0	8.2×10^{-11}	-
49	L18F3	18	3	0	1.8×10^{-5}	**0.1**

S. No.	Sample Code	Li	IL	K	Conductivity at 305 K	Capacitance at 305 K
		(mol%)			(Ω^{-1} cm^{-1})	(Fg^{-1})
50	L18F4	18	4	0	$4.7x10^{-8}$	**0.44**
51	L18F9	18	9	0	$3.3x10^{-5}$	**1.3**
52	L18F13	18	13	0	$2.2x10^{-7}$	**1.1**
Series-3						
51*	L18F4	18	4	0	$4.7x10^{-8}$	**0.44**
53	L33F4	33	4	0	$7.7x10^{-6}$	**25.4**
54	L46F4	46	4	0	0.0014	**26.5**

In order to examine the potential of these IL-based silica gel composites as supercapacitors, capacitors were fabricated using these composites as separators of electrodes. Since, the presence of IL promotes the Li^+ ion motion, as mentioned in the previous chapter, it is expected that the ionic motion at the electrode/electrolyte interface will also be facilitated. It is important to develop electrochemical supercapacitors with materials having good mechanical strength, and IL content up to certain mol % in the composites does not compromise the same. Further, in solid polymer electrolytes, it is well known that the conductivity is improved by using plasticizers that promote ionic motion. In the present systems, we can assume that the small amount of IL essentially plays the role of plasticizer.

5.3.1 [EMIM] BF_4 Containing Silica-gel Composites

5.3.1.1 Silica-gel composites having only lithium ions and no potassium ions. (Hydrolytic Process) (System 4A of Table 5.1)

To explore the potential of the composites of system 4A ([EMIM] BF_4, $LiNO_3$ confined silica gel composites prepared by hydrolytic process), in supercapacitor applications capacitance plots were determined by CV. Figs. 5.4a, 5.5a, 5.6a, and 5.7a respectively show capacitance behavior of series-1, series-2, series-3 and series-4 composites of system 4A. It can be seen that the trend for capacitance value of these composites somewhat matches with the conductivity data (discussed earlier in chapter 4).

Composites from series-1 of system 4B (for increasing Li^+ ion concentration) show an increase in capacitance with concentration of Li^+ ions. This may be due to the increased mobile ion concentration (Li^+/NO_3^-) closer to the electrode interface. It may be noted that there is a minimum concentration of the salt ($LiNO_3$) is required to see measurable capacitance value. Up to 18 mol% of lithium either negligible or very small values of capacitance are observed. The corresponding Nyquist plots do compliment the CV scans;

for series-1, Fig. 5.4b shows a higher slope for the tail in the plot. However, due to the presence of high resistance and limited (poor) conductivity, the shape of the inclined line is distorted.

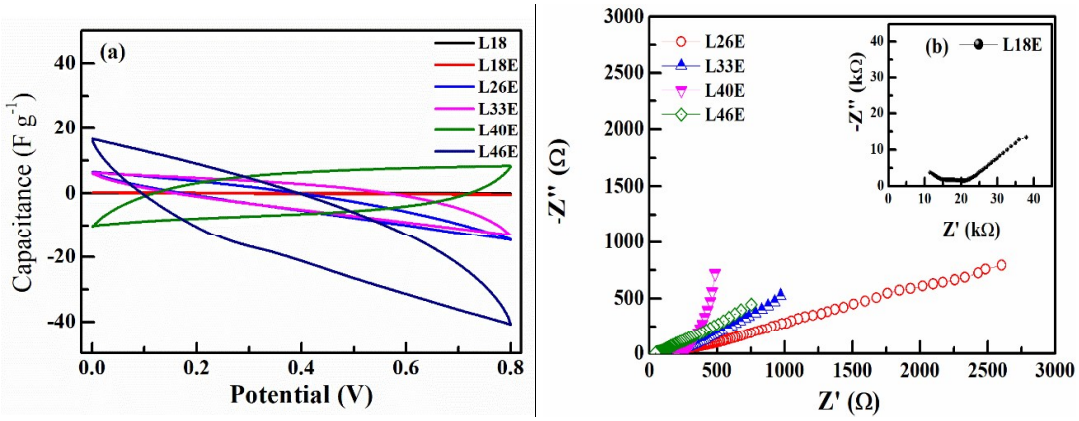

Fig. 5.4 (a) CV plots for series-1 from system 4B composites at room temperature and (b) their corresponding impedance plots for comparison.

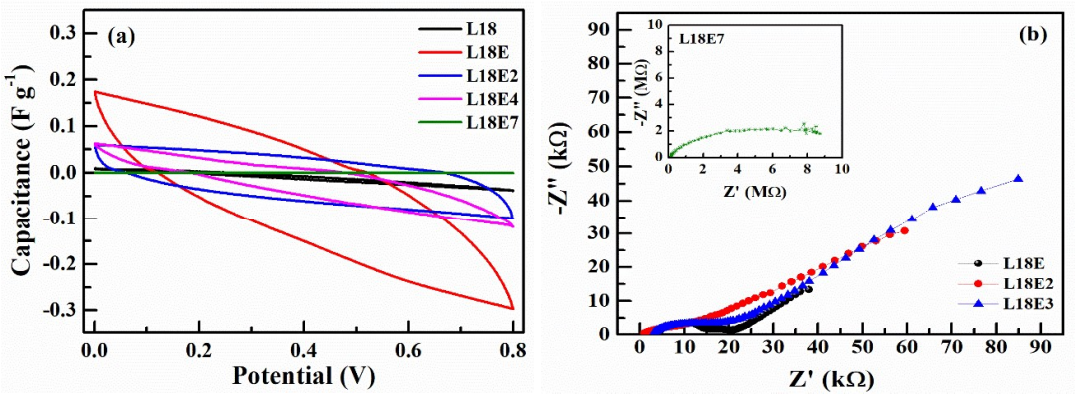

Fig. 5.5 (a) CV plots for series-2 from system 4B composites at room temperature and (b) their corresponding impedance plots for comparison.

Similarly, with an increase in IL concentration (series-2 of system 4A), capacitance of these composite decreases (Fig. 5.5a). These results do complement the conductivity trends. This is because the capability of mobile ions to form a double layer decreases as Li^+ ion may form complex with IL resulting into decrease in ion mobility. Or as an alternate explanation we may say the following: ILs increase the ionic conductivity which improves the capacitance and the same time at higher concentrations ions of IL may obstruct the pores of the activated carbon electrode. Nyquist plots of these composites are found to be

distorted with an increase in IL concentration (Fig. 5.5b). This is mainly because of increase in resistive and decrease in capacitive nature of these composites.

Again, for series-3, change in capacitance is similar to series-2. A decrease in the capacitance of the composites has been observed with increase in IL concentration. Nyquist plots (Fig. 5.6b) of the composites complement the CV scans (Fig. 5.6a), where the tail in the low frequency region of the Nyquist plot shows a higher slope. However, high resistance and limited (poor) conductivity of the composites lead to the distorted inclined line.

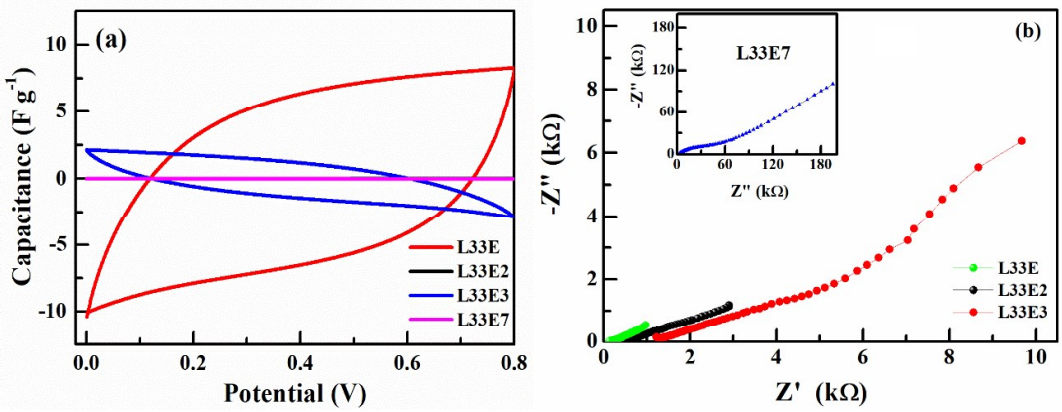

Fig. 5.6 (a) CV plots for series-3 from system 4B composites at room temperature and (b) their corresponding impedance plots for comparison.

Series-4 of the 4A system, where only IL and not the lithium salt is confined in the composites, no evidence for the charge storing ability has been observed and their corresponding CV plots exhibit almost negligible capacitance (Fig. 5.7a). Nyquist plots of these composites (Fig. 5.7b) exhibit semicircle, indicating for the absence of capacitive nature and are in agreement with the CV results. This is because the charge conducting ions are absent in these composites. Absence of fast moving mobile lithium ions in these composites prevents the formation of any double layer capacitor. This clearly marks the inability of IL ions (cation or anion) to form double layer in these solid-state silica gel composites and this may be due the mismatch of pore size of electrode material with that of the ion size of ILs components.

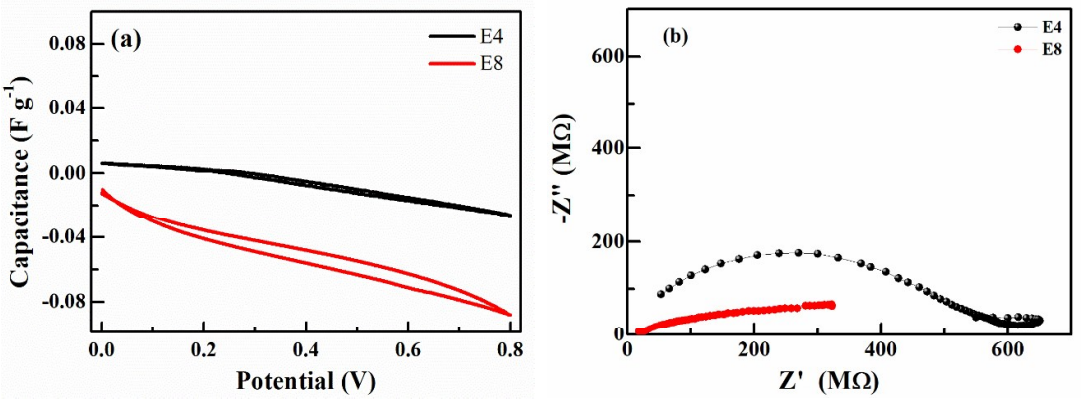

Fig. 5.7 (a) CV plots for series-4 from system 4B composites at room temperature and (b) their corresponding impedance plots for comparison.

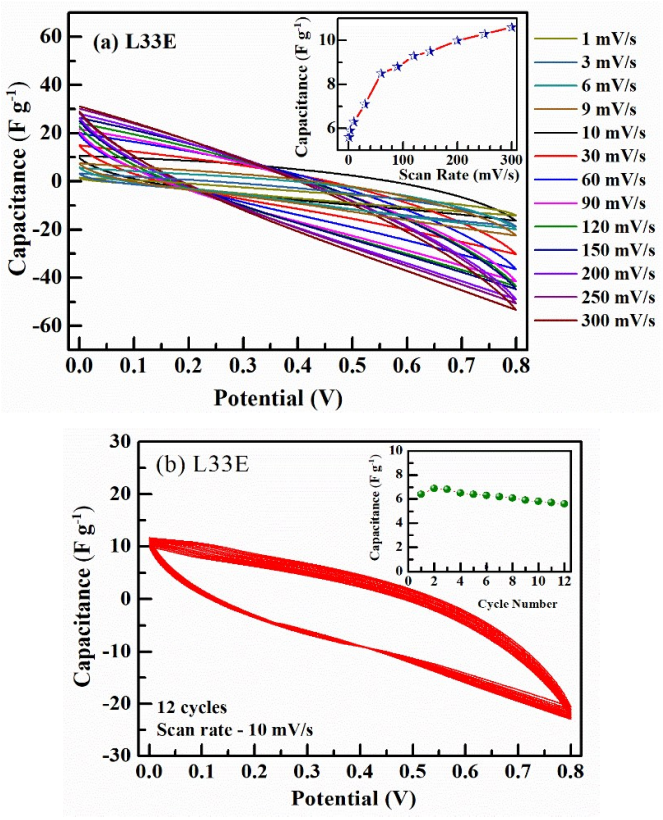

Fig. 5.8a Capacitance of L33E composite with change in Scan rate. Inset: A systematic increase in capacitance with Scan rate is evident. Fig. 5.8 b Consequtive 12 CV cycles of L33E composite. Inset: Capacitance variation is negligible up to 12 cycles.

To further assess the performance of the capacitors fabricated with silica gel composite as electrolyte, the capacitance values were obtained as a function of cycles and scan rate in

cyclic voltammetry. Fig. 5.8a shows CV cycles at different scan rates. As evident, the area under the curve shows a systematic increase that suggests larger charge storage. Thus, capacitance increases rapidly for higher scan rates. Higher scan rate leads to longer diffiusivity for ions due to which they can migrate inside the pores of the electrodes. In addition, a larger fraction of mobile ion concentration can be influenced when higher scan rates are applied [11-12]. In Fig. 5.8b, we see for almost 12 cycles the area under the curve, and hence charge storage, remains constant. This suggest a good reversibility and good charge storage ability of the device. Highly reversible and stable capacitance also suggests that the IL and salt confined silica gel electrolytes provide faster ion transport across the interface.

Fig. 5.9 shows the variation of conductivity(RT) and capacitance with the change in the concentration of confined lithium salt. The trend is similar and comparable.

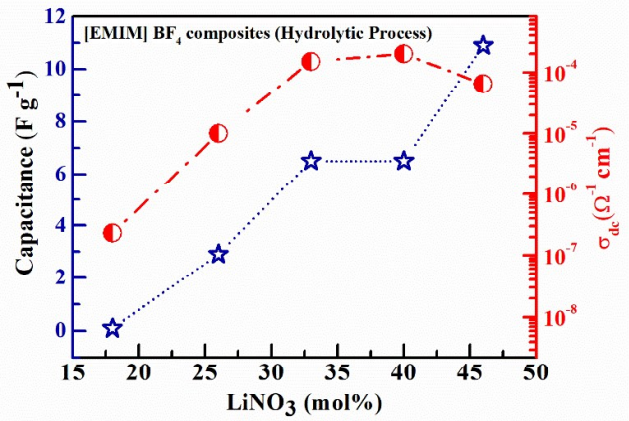

Fig. 5.9 Comparison of Capcitance change with that of conductivity (RT) with Li salt concentration variation for the composites of series-1

These observations are summarised as follows: (i) High diffusion of Li^+ ions across the electrolyte-electrode interface results in an increase in capacitance of the composites of series-1 (with increase in Li^+ ion concentartion). (ii) Series-2 and series-3 samples (with high IL mol %) exhibit negligible capacitance. These samples exhibit a decrease in capacitance with an increase in IL concentration. (iii) Only IL confined samples (series-4) showed negligible/no capacitance due to absence of Li^+ ions. (iv) L33E composite shows stable capacitance for many cyles (tested for 12 cycles); and this may be true for other composites also.

5.3.1.2 Silica-gel composites having both lithium and potassium ions (Hydrolytic Process) (System 4B of Table 5.1)

The system 4B has been fully explored for conductivity in chapter 4 and the focus was mainly to understand the mixed alkali effect. If K^+ ions replace all Li^+ ions (series-3) in sol-gel derived silica-gel composites (with the same activated carbon electrode used in the previous section) exhibit almost zero capacitance (Fig. 5.10a). This may be due to the pore size of the activated carbon is not matching with the ion size of potassium. The corresponding Nyquist plots (Fig. 5.10b) also indicate increased resistive nature.

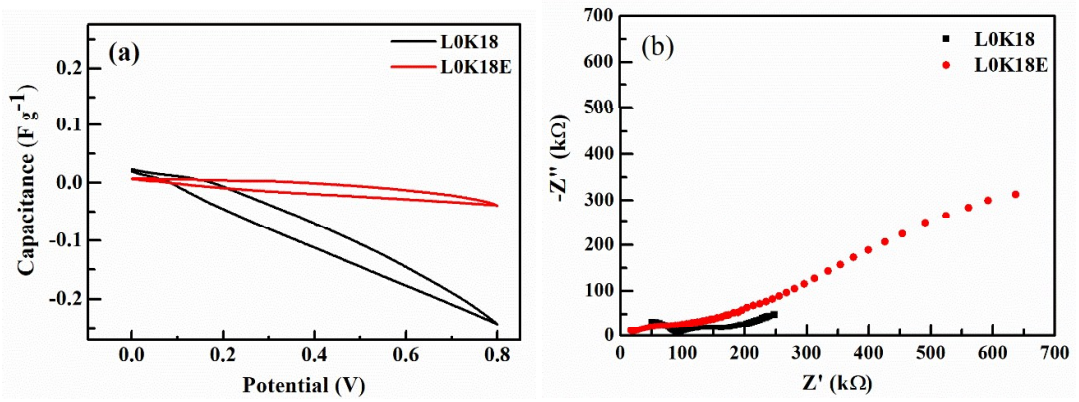

Fig. 5.10 (a) CV plots for only K^+ ion containing composites (series-4- system 4c) at room temperature and (b) their corresponding impedance plots for comparison.

Composites of 4B series-1 are prepared by substituting 50% of lithium ions by potassium ions in the 4A series-1 composites. Thus L18 and L18E composites with 50% substitution are labeled as L9K9 and L9K9E respectively. No appreciable change in the capacitive property of the composites has been seen compared to the total lithium ion composite (Fig. 5.11a). The same is well supported by high resistance in Nyquist plots (Fig. 5.11b). Here we should note that above 18 mol% of the lithium ions are required to show any measurable capacitance in the composites where the IL is [EMIM] BF_4. Thus it is not expected to have

any impact on capacitance when the total alkali ion content is less than or equal to 18 mol %.

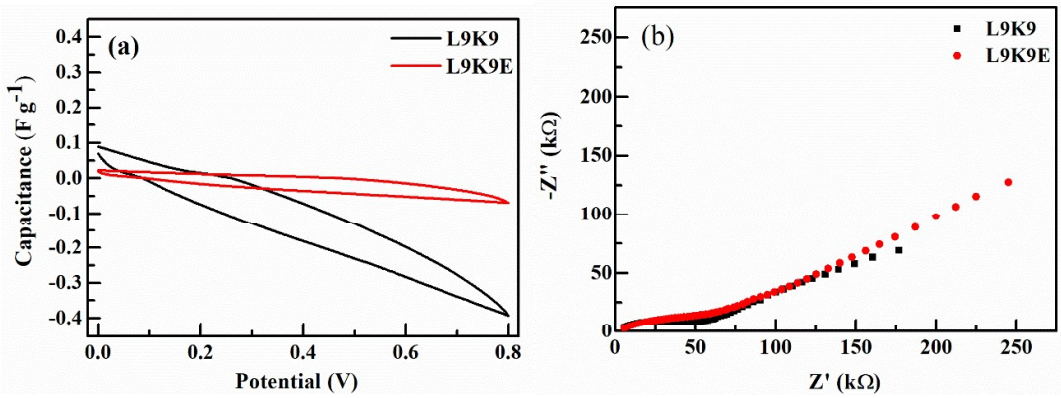

Fig. 5.11 (a) CV plots for 50% K^+ion substitution in Lithium containing silica gel composites (discussed in section 5.2.2.1 for L18 and L18E) at room temperature and (b) their corresponding impedance plots for comparison.

System 4B series-1 composites were prepared such that total alkali ion concentration is varied keeping lithium ion to potassium ion ration almost 1:1. Except for the case where the total alkali ion concentration is 18 mol % in all other composites the capacitance decreases drasitcally compared to the corresponding 'lithium ion only' cases. Representative CV and Nyquist plots are shown in Fig. 5.12. Although these compoistes are marked with high resistance, but with increase in ion concentration, Nyquist plot marks for a decrease in resistance of the composites (Fig. 5.12b). Surprisingly, the change in conductivity and the change in capacitance for varied concentrations of potassium ions show different trends. The conductivity changes are opposite to that of "mixed alkali effect" reported for traditional glass systems and in some of the composites conductivity increases with potassium substitution. This has been explained in Chapter 4. On the other hand the substitution of lithium by potassium decreases the capacitance. Since both capacitance measurements were done with the same activated carbon electrode it is reasonable to say that the pore size of the electrode is not matching with that of potassium ion size, thus hindering the double layer formation. Measurements with activated carbon of higher pore size can confirm this assumption.

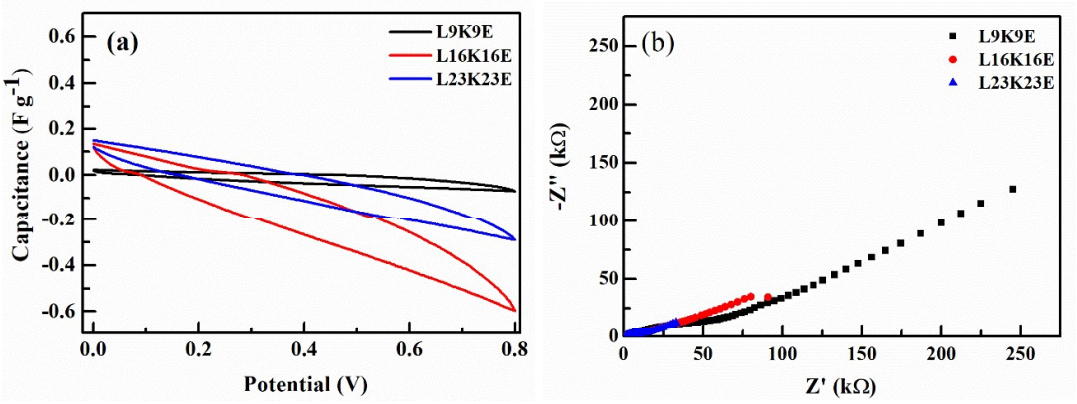

Fig. 5.12 (a) CV plots for series-2 from system 4C composites at room temperature and (b) their corresponding impedance plots for comparison.

To further probe the role of individual ions (Li^+, K^+) ion in formation double layer of capacitance, composites of series-2 of system 4B were prepared. In this series-the composties were prepared with compositions same alkali ion content as that of L18E, L23E, and L36E of system 4A but with lithium content reduced to 9 mol % in all three cases by replacing lithium with potassium.

The CV plots (Fig. 5.13a) and the calculated capacitance value compared with the corresponding composites of series-4A show that potassium substittution drastically reduces the capacitance values. High resistance and lower capacitance of these composites is seen in their Nyquist plots also(Fig. 5.13b).

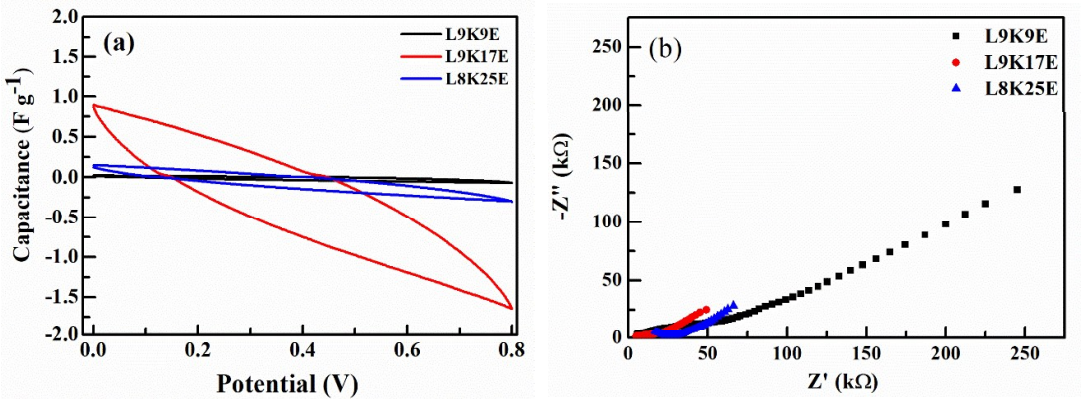

Fig. 5.13 (a) CV plots for series-3 from system 4C composites at room temperature and (b) their corresponding impedance plots for comparison.

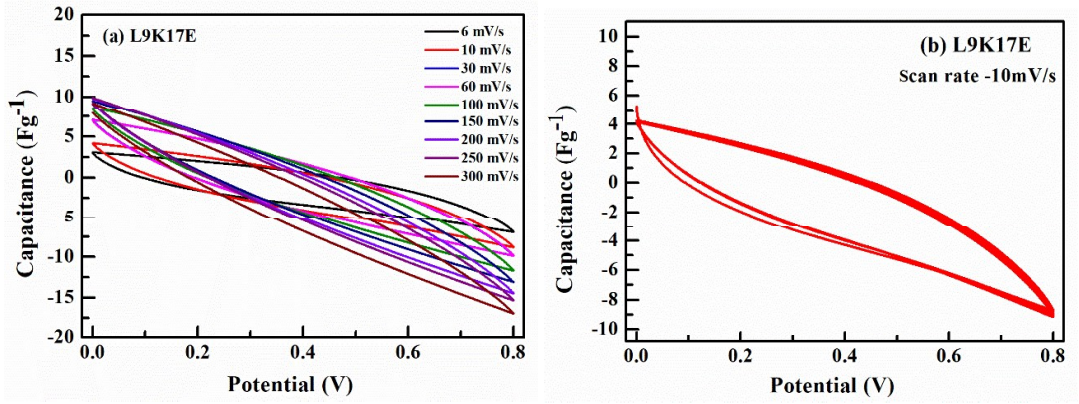

Fig. 5.14 (a) Capacitance of L9K17E composite with change in Scan rate. (b) Consequtive 12 CV cycles of L9K17E composite.

Even though the composites of the system 4B are of low capcitance values, for one of the composites, L9K17E, we wanted to check the effect of scan rate variation and repeatability of the cycles. Fig. 5.14a shows CV cycles at different scan rates. The area under the curve shows a systematic increase that suggests charge storage. Thus, capacitance increasese rapidly for higher scan rates. as explained above [11,12]. CV scans for almost 12 consequtive cycles showed almost constant charge storage, indicating for good reversibility and good charge storage ability of the device.

These observations may be summarised as follows: Compared with system 4A composites, the potassium substitution of lithium in system 4B reduces the capacitance in all the cases. This is due to mismatch of potassium ion size with that of the pore size of electrode material (activated carbon). This requires confirmation by performing experiments of activated carbons of different pore sizes.

5.3.1.3 Capacitance for Li^+ ion containing silica gel composites (Non-hydrolytic Process). (System 4C of Table 5.1)

We have also synthesized all the composites of system 4A by a non-hydrolytic sol-gel process as mentioned in the previous chapter. The capacitance studies for these $LiNO_3$, and [EMIM] BF_4 containing silica gel composites (system 4C) were done and the results are presented below.

Capacitance for series-1 (for increasing Li^+ ion concentration) composites, are very low compared to the composites prepared by hydrolytic route (Fig. 5.15a). Their corresponding

Nyquist plots do compliment the CV scans (Series-1, Fig. 5.19a) where high resistance and lower capacitance is seen.

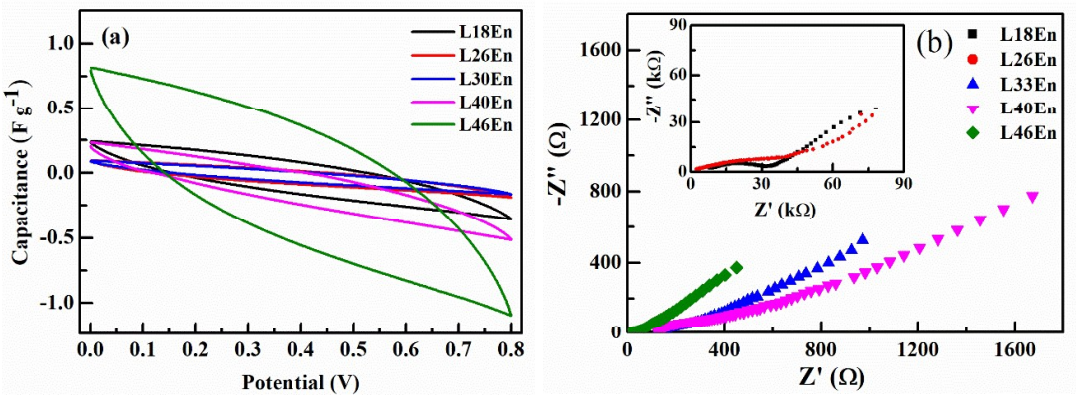

Fig. 5.15 (a) CV plots for series-1 (system 4C) composites at room temperature and (b) their corresponding impedance plots for comparison.

Similarly, for series-2 (system 4C), for an increase in IL concentration further decrease in capacitance of these composites was observed (Fig. 5.16a). Nyquist plots of these composites are found to be distorted (Fig. 5.16b).

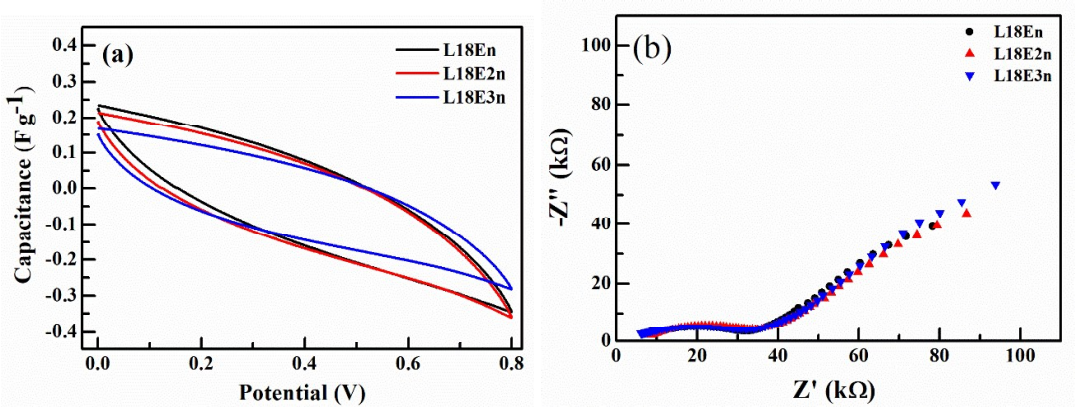

Fig. 5.16 (a) CV plots for series-2 from system 4C composites at room temperature and (b) their corresponding impedance plots for comparison.

CV plots for Series-3 (system 4C) composites again show lower capacitance compared with their hydrolytic process counter parts (system 4A) (Fig. 5.17a). The corresponding Nyquist plots of these composites do compliment the CV scans (Fig. 5.17b). Presence of depresed semicircle in high frequency region for L33E3n and L40E3n composites is a clear

evidence of the resistaive nature. However, an inclined line for Nyquist plot of L46E3n composite can be observed corresponding to its capacitance behavior.

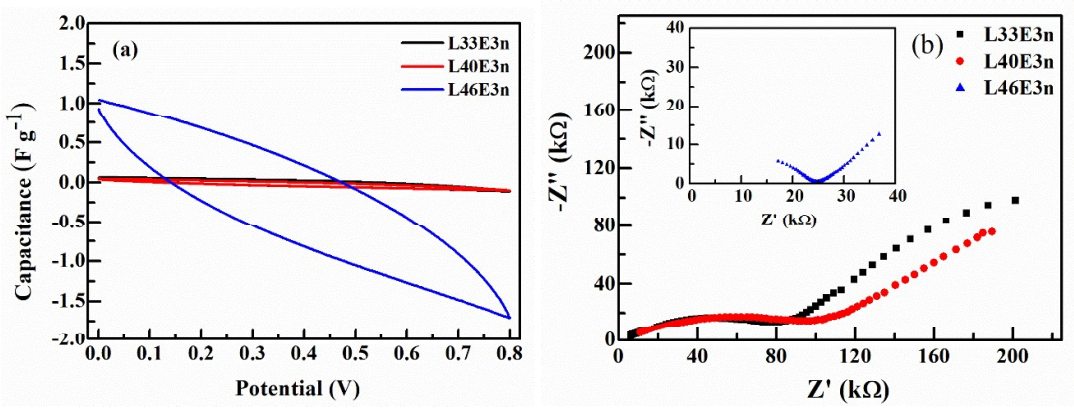

Fig. 5.17 (a) CV plots for series-3 from system 4C composites at room temperature and (b) their corresponding impedance plots for comparison.

The reproducitbility and stability performances of the capacitor cell was determined by performing CV at different scan rates as well as with time for L46En composite (Fig. 5.18).The capacitive performances for L46En composite observed at different scan rate showed no normal capacitive nature. As it has been mentioned above, it is expected that there is an increase in capacitance of the composites with increase in scan rate. No such observation was noticed for L46En composite. This clearly showed that the compoistes derived from non-hydrolytical sol-gel process do not exhibit any significant capacitance. Thus, are unsuitable for supercapacitor device applications.

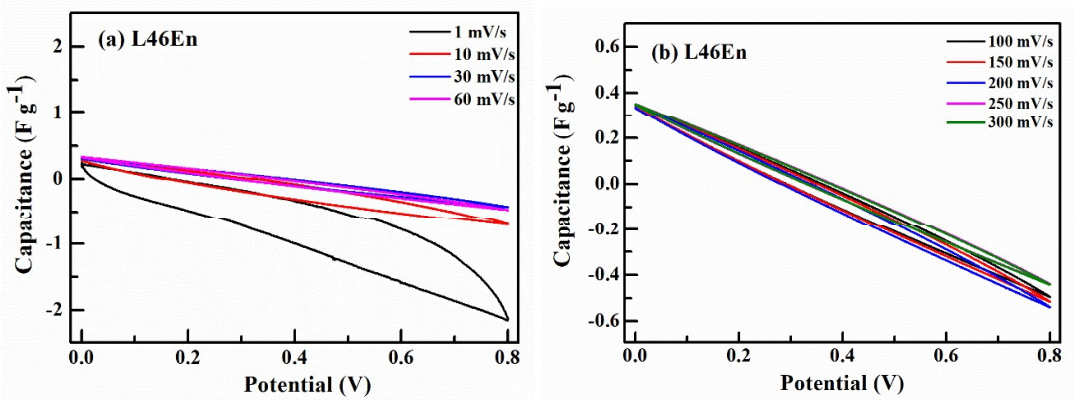

Fig. 5.18 Capacitance of L46En composite with variable scan rates.

Also CV scans repeated for 12 consequtive cycles showed no stability in the charge storage (Fig. 5.19).

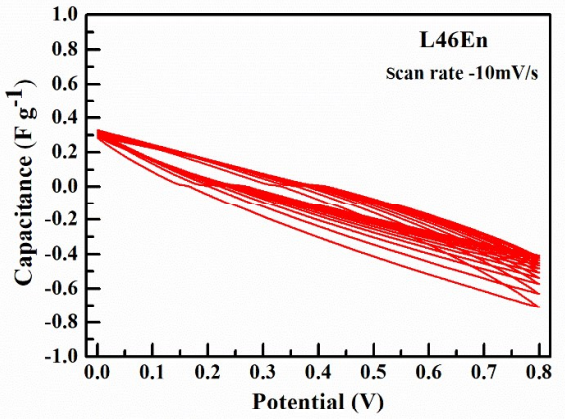

Fig. 5.19 Consequtive 12 CV cycles of L46En composite.

The main difference in the products obtained from hydrolytic and non-hydrolytic sol-gel process is the solvent filling the nano-pores of the gel. In the case of hydrolytic route ethanol-water mixture is filled in the ultrapore and in nonhydrolytic process it the formic acid which has a low ionization constant. Also the presence of silanol (Si-OH) groups will be much higher in hydrolytic synthesis compared to the non-hydolytic route. We find system 4C (non-hydrolytic) composites show low conductivity and low capacitance (almost nil) compared to system 4A composites. Thus it shows the ethanol water mixture in the ulrapores of gels and silanol groups are essential for conductivity and capacitance of the silica gel composites. Finally we conclude this section by saying Li^+ ion containing composites from non-hydrolytic sol-gel process are not suitable for supercapacitor device applications.

5.3.2 [BMIM] Br containing silica gel composites (System 4D of Table 5.1)

Electrochemical characterization of these composites has been done using two-electrode cell and by cyclic voltammetry (CV) at room temperature with a scanning rate of 0.01 V/sec. Fig. 5.20 shows the cyclic voltammogram of some of the composites. The capacitance of the cells can be obtained from the cyclic voltammograms as, C = i/s, where, "i" is the average current and "s" is the potential sweep rate. A reversible charge-discharge behavior of the composites has been observed.

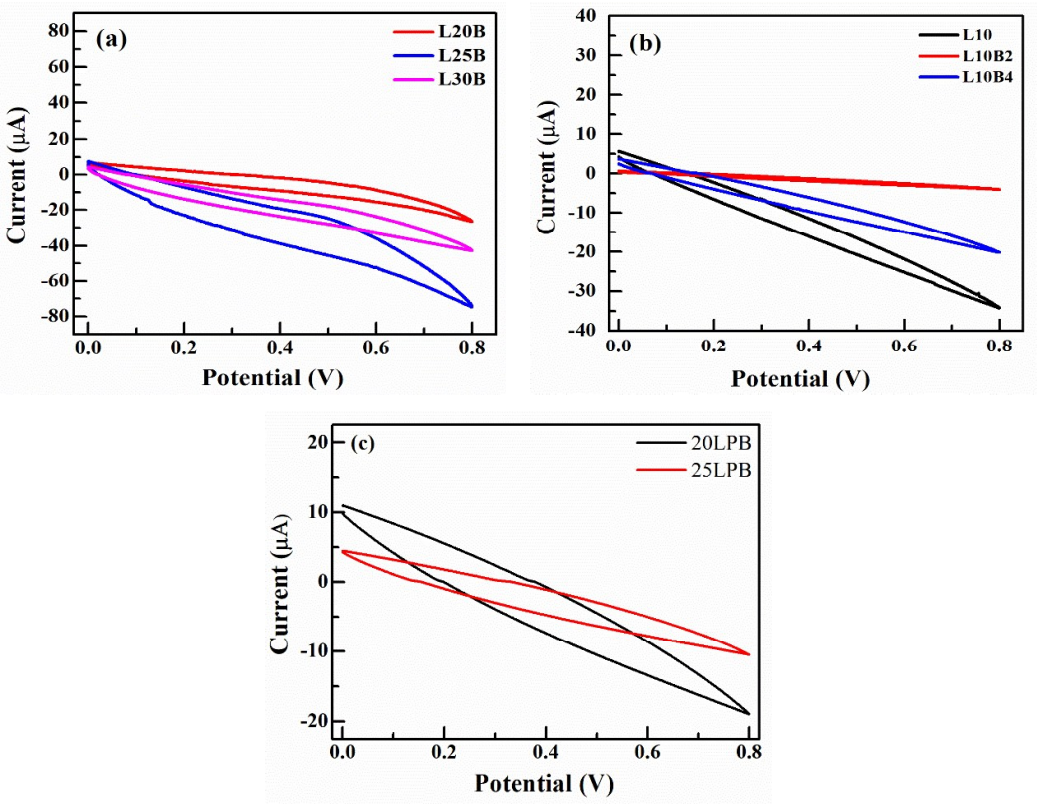

Fig. 5.20 Cyclic-voltammogram of capacitors with different composites as separators (a) series-1 (b) series- 2 and (c) series-3

Nyquist plots of some of the composites are given in Fig. 5.21. These do compliment the CV scans. The substantial capacitance value is noticed for the samples (Series-1, Fig. 5.20a) where the tail in the Nyquist plot shows a higher slope. However, due to the presence of high resistance and limited (poor) conductivity, the shape of the inclined line is distorted (scattered). Apparently, the cyclic voltammogram for Series-1 appeared almost parallel to zero current line, which is indicative of capacitive charge storage. In the case of series-2 samples, due to high resistivity, no specific trend in the impedance spectra is observed, which is restricted by very low conductivity values of the order of 10^{-10} Ω^{-1} cm^{-1}. Since the ions are not mobile to form a double layer, the corresponding capacitance values are relatively poor (Table 1).

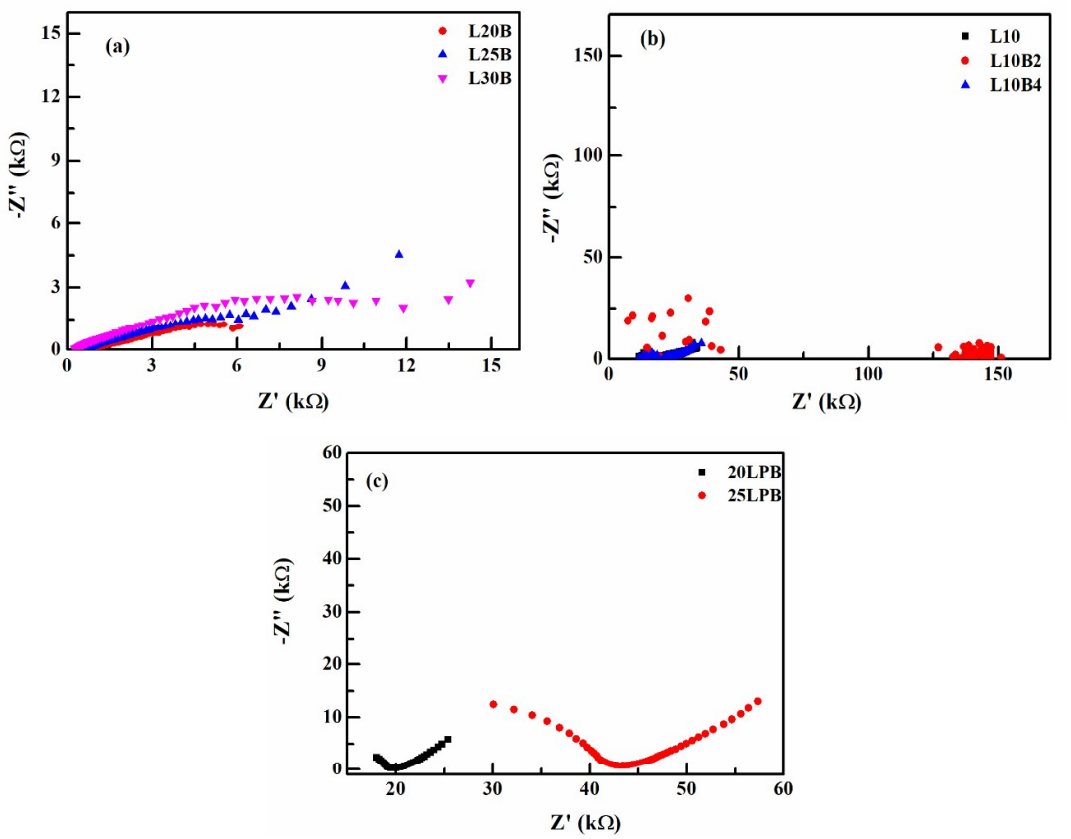

Fig. 5.21 Impedance plots for capacitors with different composites (a) series-1 (b) series- 2 and (c) series-3

For series-3, again a tail at lower frequencies is observed. However, its corresponding capacitance is relatively low. The CV scan for series-3 is diagonally tilted, that may be due to non-capacitive (reactive) charge storage owing to some electrochemical reactions brought in by the addition of lead nitrate. Preliminary findings of average capacitance are shown in Table 5.1.

The three series-have composition variation as follows: Series-1 –No lead, IL concentration is fixed and lithium concentration is varied; Series-2 – No lead, lithium concentration is fixed and IL concentration is varied; Series-3 – Lead is fixed at 10 mol%, IL concentration is fixed and lithium concentration is varied.

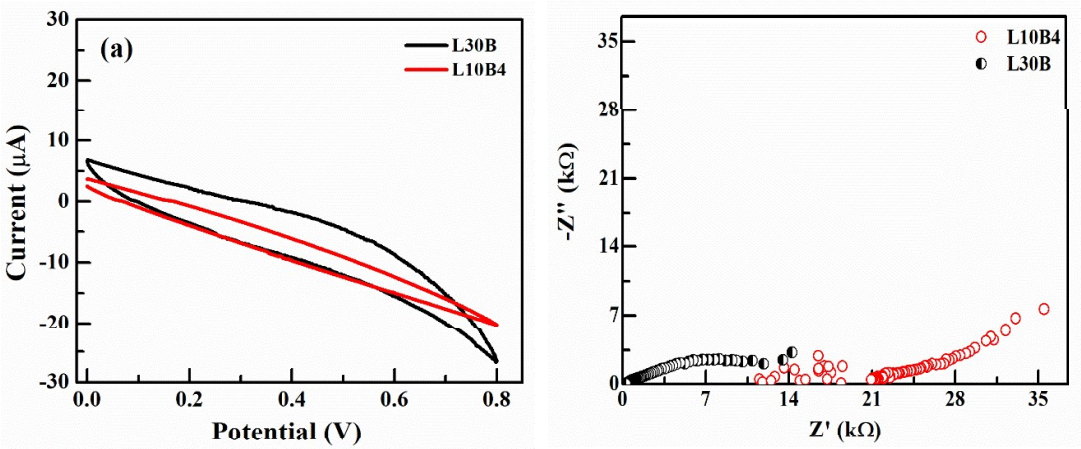

Fig. 5.22 CV plots for L10B4 and L30B composites (left) at room temperature and their corresponding impedance plots (right) for a comparison.

Fig. 5.22 shows the CV and IS curves of the composite showing maximum capacitance (30LB) along with that of showing negligible capacitance (10L4B). The difference in current values between forward and reverse sweep of voltage happens to be high for composites with high Li^+ content.

It is observed that: (i) Increase in capacitance with Li^+ ion content (series-1) is attributed to the high diffusion of Li^+ ion across the electrode-electrolyte interface. The exposed surface area is easily accessible to Li^+ ions, which form the electrical double layer with polarizable carbon electrodes. However, above 20 mol% of lithium salt in the composite is required to show any appreciable capacitance value. (ii) Series-2 samples (with high IL mol %) exhibit negligible capacitance. Essentially this tells us that unless the lithium concentration is above the threshold value, increase in IL concentration is not going to improve the capacitance. IL addition improves ionic conductivity of lithium as seen in chapter 4. Upto a certain mol% of IL the improvement of ionic conduction helps in increasing the capacitance; however, when additional IL is added the bigger ions arising from the IL may block the pores of carbon electrode due to mismatch in size. (iii) Introduction of a heavy metal ion such as Pb^{2+} in the matrix (series-3), reduces the capacitance. This may be due to the mismatch of ion size with pore size of carbon electrodes.

5.3.3 Capacitance from IL: [EMIM] CF_3SO_3 containing composites (System 4E of Table 5.1).

The effect of change in IL anion ([EMIM] CF_3SO_3) on the capacitance behavior of silica gel composites was determined. Fig. 5.23a, 5.24a, and 5.25a show capacitance behavior of series-1, series-2, and series-3 composites (Chapter 4 - System 4E) respectively.

With increase in Li^+ ion concentration, increase in capacitance was observed (Fig. 5.23a). This is an evident for the formation of double layer with increase in mobile ion concentration. Their corresponding Nyquist plots (Fig. 5.23b) further supported these results. From these CV plots, it is interesting to note that the capacitance of these composites are substantially higher than the corresponding composites containing IL [EMIM] BF_4 (system 4A).

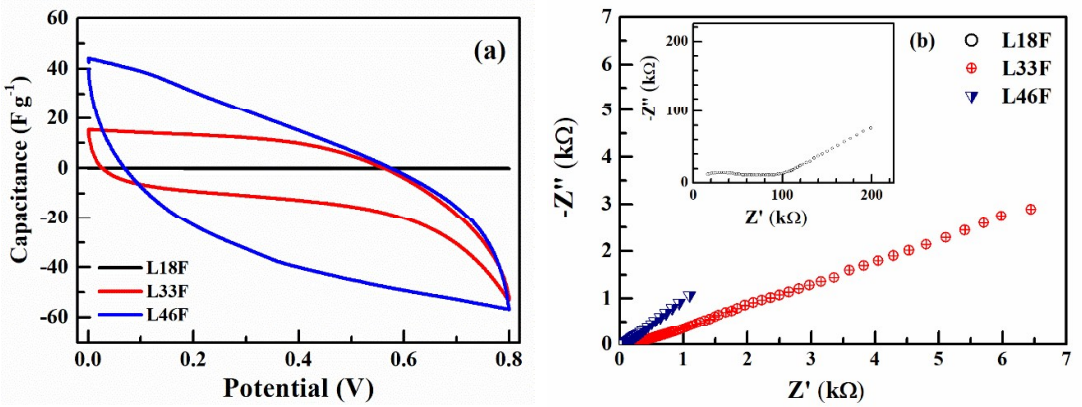

Fig. 5.23 (a) CV plots for series-1 (system 4E) composites at room temperature and (b) their corresponding impedance plots for comparison.

Fig. 5.24a shows the CV plots for composites with increasing IL concnetration. Unlike, sytem 4A (anion BF_4^-), we find some change in capacitance with increase in IL concentration. However, there is no trend, and these capacitance values are still low as compared to higher amount of Li^+ ion containing composites. As stressed earlier in the discussion of other series, we find lithium ion concentration should be above 18 mol % to obeserve substantial capacitance value. Nyquist plots of these composites are found to exhibit inclined nature supporting for the formation of capacitor layer at the interface. However, its distorted nature for L18F and L18F3 composites is basically due to the resistive nature of the composites (Fig. 5.24b).

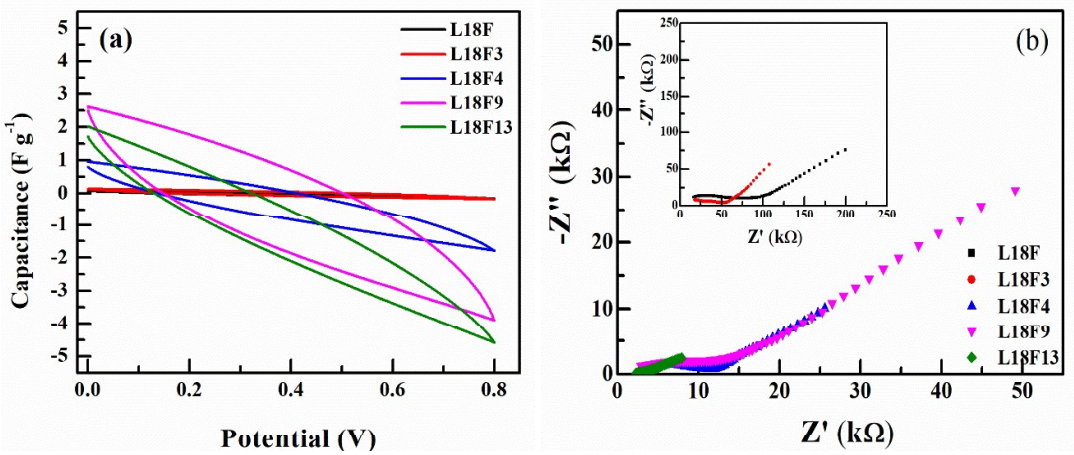

Fig. 5.24 (a) CV plots for series-2 (system 4E) composites at room temperature and (b) their corresponding impedance plots for comparison.

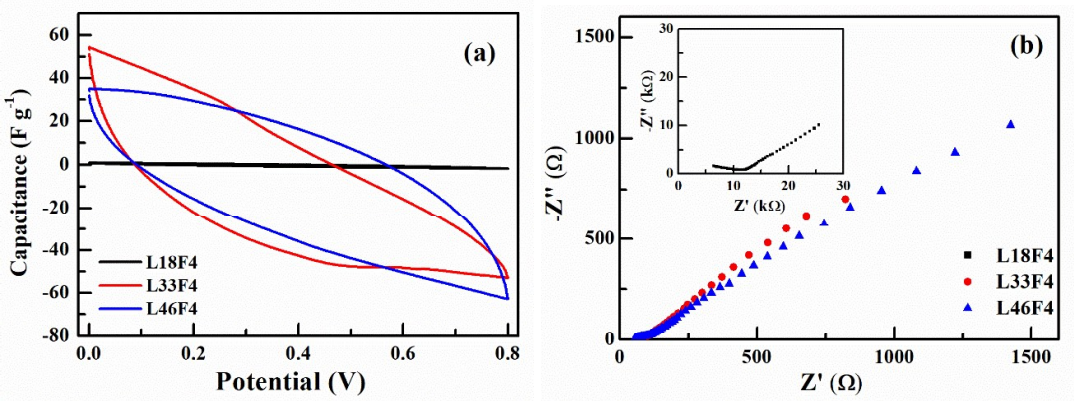

Fig. 5.25 (a) CV plots for series-1 from system 4E composites at room temperature and (b) their corresponding impedance plots for comparison.

An increase in capacitance has also been noticed for series-3 (system 4E) where keeping the IL concentration at 4 mol % the lithium ion concentration is varied. The CV results support for increased mobile charge carriers (Fig. 5.25a) and their corresponding Nyquist plots supports the formation of capactiance at the interface (Fig. 5.25b). As seen in other systems here also we find substantial increase is seen only for composites having lithium concentration more than 18 mol %. It is also interesting to note when lithium ion concentration is maintained at 33 mol % increase in IL concentration from 1 to 4 mol% increases the capacitance whereas exactly the reverse happens when lithium ion concentration is 44 mol %. This may indicate complex formation between IL and lithium ions.

The capacitance values were obtained as a function of cycles and scan rate in cyclic voltammetry in order to assess the performance of the capacitor. Fig. 5.26a shows CV cycles at different scan rates. As evident, the area under the curve shows a systematic increase with scan rate that suggests larger charge storage. Higher scan rate leads to longer diffiusivity for ions due to which they can migrate inside the pores of the electrodes. In addition, a larger fraction of mobile ion concentration can be influenced when higher scan rates are applied [11, 12]. Further, as shown in Fig. 5.26b, for almost 12 cycles the area under the curve, and hence charge storage, remains constant. This suggest a good reversibility and good charge storage ability of the device. Highly reversible and stable capacitance also suggests that the silica gel electrolyte provides faster ion transport across the interface.

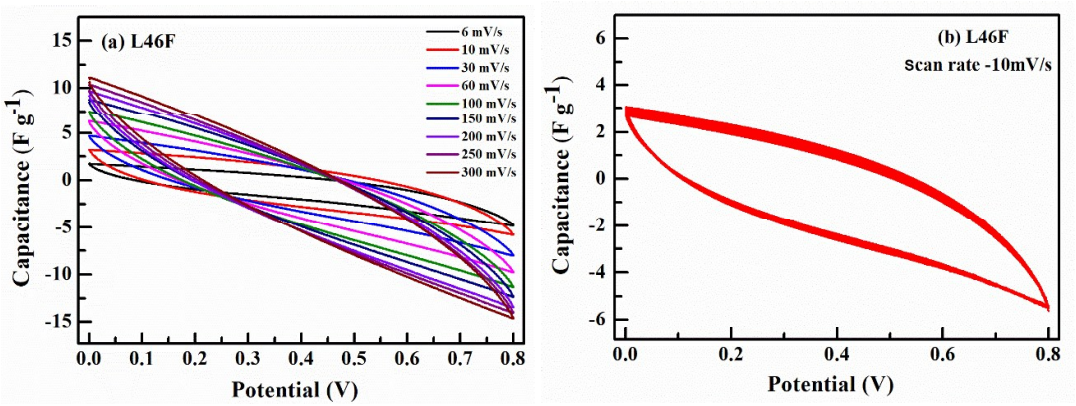

Fig. 5.26 (a) Capacitance of L46F composite with change in Scan rate. (b) Consequtive 12 CV cycles of L46F composite.

Again driven by curiosity we have tested the high temperature performance of one of the composites (L46F) which has a good capacitance value, as high temperature electrical conductivity of the sol-gel derived silica gel composites has been explored in the previous chapter. The tempearture dependance on CV plots was analyzed.

Fig. 5.27 shows, variation in capacitance of L46F with temperature. It was intersting that the initial capacitance could be maintained significantly up to 100 ^{o}C with a peak value at 50 ^{o}C. Howerver, with further increase in temperature, the capacitance values decreases drastically and showing zero capacitance at 200 ^{o}C. At further higher temperatures i.e. beyound 200 ^{o}C, these composites again exhibit steady and substantial capacitance.

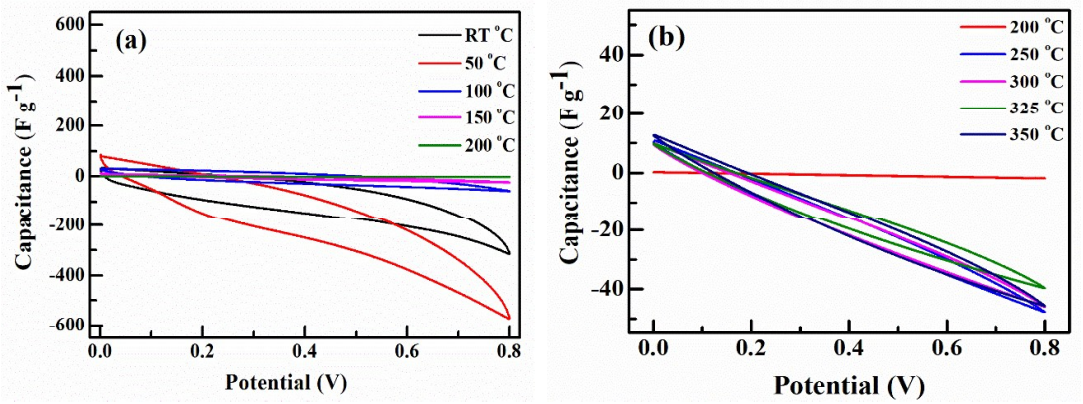

Fig. 5.27 Capacitance of L46F composite with temperature variation.

Table 5.2 Capacitance variation at high temperatures for L46F composite:

Temperature (^oC)	35	50	100	150	200	250	300	325	350
Capacitance (Fg^{-1})	84	164	19	7	0	18.7	18.6	16.2	17.8

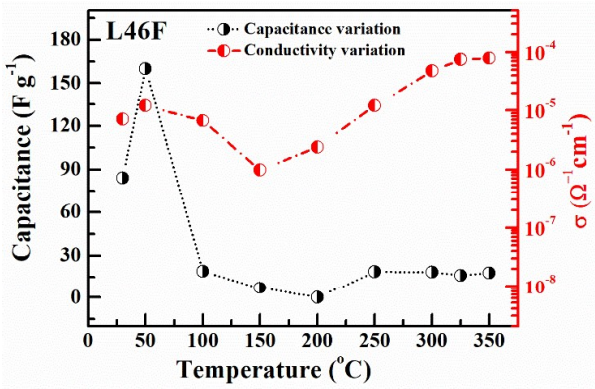

Fig. 5.28 Capacitance of L46F composite with temperature variation.

The results indicate that these composites can also be suitable for high temperature, solid-state device applications. However, this needs thorough optimization and further investigations.

In summary we may say that the anion change in the IL from BF_4^- to $CF_3SO_3^-$ brings in substantial increase in capacitance. Other trends remain the same as series 4A. These composites also show capacitance up to 18 F g^{-1} in the temperature range of 250 ^oC to 350 ^oC.

5.4 Anamolous behavior of Nyquist plots

In the above discussion we have stated many times that the CV and Nyquist plot information is matching. Anamolous behavior of Nyquist plots are briefly discussed below; Anamolous Nyquist plots (small semicircle in high frequency region followed by inclined line/verticle spike in low frequency region) is observed for cells of ceratin composites; and this could be due to poor charge storing ability of such composites. In these composites, such a phenomenon is indicative of low charge-transfer resistance and a pronounced capacitance behavior with small diffusion resistance. Semicircle obatined at mid frequencies is characterized by charge transfer resistance (R_{CT}) and the associated double layer capacitance (C_{dl}) [13]. Low frequency inclined line corresponds to Wurburg slope line, which represents semi-infinite diffusion of Li^+ ion in the electrodes.

Also we find in literature [14] that in the Nyquist plots the presence of depressed semicircle in high frequency domain (Fig. 5.29), indicates the presence of Warburg element. It described the structural and geometric inhomogeneities in diffusion path of Li^+ ions on intercalation with the electrode material.

Shown below (Fig. 5.29) are the Nyquist diagrams and the corresponding equivalent circuit obtained by fitting the data with a popular software (Z-view).

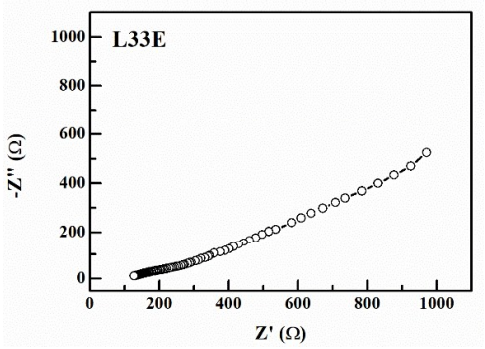

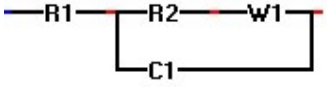

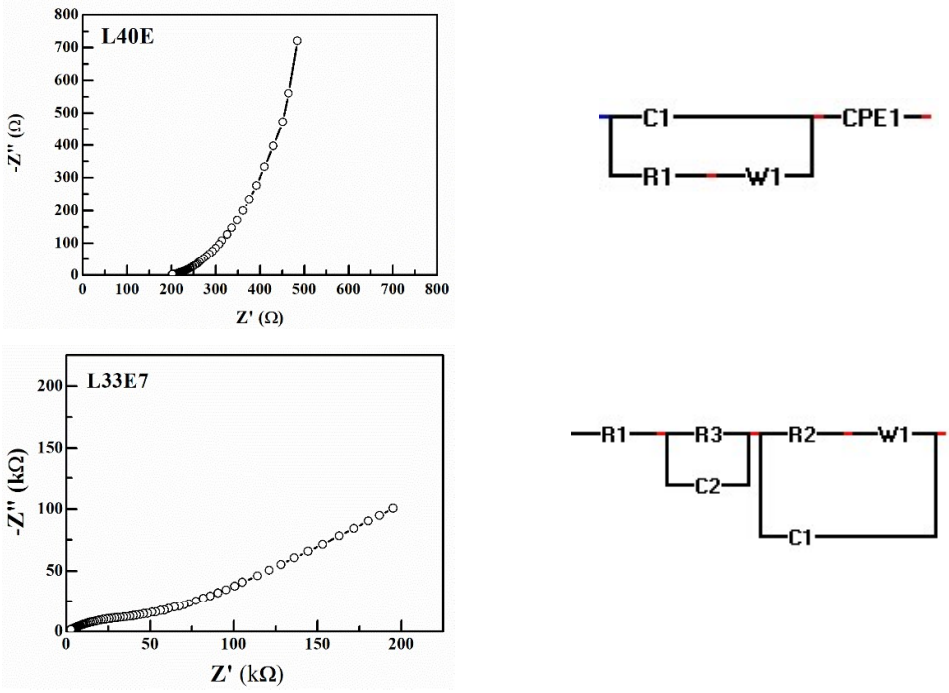

Fig. 5.29 Impedance plots for (a) L33E, (b) L40E and (c) L33E7 composites, corresponding equivalent circuits are also mentioned.

5.5 Conclusion

We have identified the IL and lithium salt confined silica gel compoistes are potenital solid state electrolytes and super capcitor cells can be built based on these electrolytes. Even though the capacitance for these composites is not very high in comparison to gel polymer-based electrolytes, the potential to manipulate the composition with a variety of ILs and through that capacitance is indeed encouraging. Choice of suitable high surface area electrodes may give better results and further studies in this direction are needed. Some of the important conclusions drawn form above investigations are:

i. Increase in capacitance of the composites are generally observed for increase in Li^+ in concentration. High capacitance may be attributed to high diffusion of Li^+ ions across the electrode-electrolyte interface. The exposed surface area is easily accessible to Li^+ ions, which form the electrical double layer with polarizable carbon electrodes. However, below a minimum threshold value of lithium ion concentration (20 mol%) it is not possible to observe any detectable capacitance.

ii. Increase in the concentration of IL above a particular value (1 mol%) generally decreases the capacitance. We find that unless the lithium concentration is above

the threshold value, increase in IL concentration is not going to improve the capacitance. IL addition improves ionic conductivity of lithium as seen in chapter 4. Upto a certain mol% of IL the improvement of ionic conduction helps in increasing the capacitance; however, when additional IL is added the bigger ions arising from the IL may block the pores of carbon electrode due to mismatch in size and thus reduce the capacitance.

iii. Very low (by orders of magnitude) capacitance could be observed for silica gel composites confining only the IL and no alkali metal ion. This indicates the presence of mobile ion (alkali metal ions such as Li^+ , K^+ etc.) is necessary for double layer formation.

iv. Introduction of a heavy metal ion such as Pb^{2+} or different sized alkali ion such as K^+ reduces the capacitance. This is due to mismatch of the bigger ion's size with that of the pore size of electrode material (activated carbon). This requires confirmation by performing experiments of activated carbons of different pore sizes. On the other hand one may use this characteristic to tune the capacitance values by using appropriate amounts of heavy metal ions doped in these composites for device applications.

v. Li^+ ion (or other alkali ion) containing composites prepared by non-hydrolytic sol-gel process are not suitable for supercapacitor device applications. In the case of hydrolytic route ethanol-water mixture is filled in the ultrapore and in nonhydrolytic process it the formic acid which has a low ionization constant. Also the presence of silanol (Si-OH) groups will be much higher in hydrolytic synthesis compared to the non-hydolytic route. We find non-hydrolytic route composites show low conductivity as well as low capacitance almost nil compared to similar composites obtained through hydrolytic route. Thus it shows the ethanol water mixture in the ulrapores of gels and silanol groups are essential for conductivity and capacitance of the silica gel composites.

vi. Capacitance of the composites exhibit good reproducibility as well as stability when cheked upto 12 cycles. The observed capacitance value increases with increae in scan rates [15]

vii. We also observe the anion change in the IL from BF_4^- to $CF_3SO_3^-$ brings in substantial increase in capacitance. Other trends remain the same as in other

systems. This increase may be due to the lower viscosity of the IL ([EMIM] CF_3SO_3) and the increased ionic conductivity of Li^+ ions [16].

viii. High temperature capacitance measurements of L46F composite showed almost steady capacitane values (up to 18 Fg^{-1}). These systems can be tuned and optimised for high temperature supercapacitor solid-state devices in the temperature range 250-350 ^oC. It may be noted that we find super capcitor high temperature capacitance measurements have been done in polymer based systems, however, the highest temperature used in the experiments are around 120 ^oC only [17].

References

1. M. Vangari, T. Pryor, L. Jiang, "Supercapacitors: Review of materials and fabrication methods", *Journal of Energy Engineering* **139** (2013) 72-79.
2. Zengxin Dai, Chuang Peng, Jung Hoon Chae, Kok Chiang Ng, George Z. Chen, "Cell voltage versus electrode potential range in aqueous supercapacitors", *Scientific Reports* **5** (2015) 5884.
3. Cheng Zhong, Yida Deng, Wenbin Hu, Jinli Qiao, Lei Zhang, Jiujun Zhang, "A review of electrolyte materials and compositions for electrochemical supercapacitors", *Chemical Society Reviews* **44 (**2015) 7484-7539.
4. Jocelyn E. Zuliani, Johnathon N. Caguiat, Donald W. Kirk, Charles Q. Jia, "Considerations for consistent characterization of electrochemical double-layer capacitor performance", *Journal of Power Sources* **290** (2015) 136-143.
5. Xiaoming Ge, Changjing Fuab, Siew Hwa Chan, "Double layer capacitance of anode/solid-electrolyte interfaces", Physical Chemistry Chemical Physics **13** (2011) 15134–15142.
6. Khu Le Van, Thu Thuy Luong Thi, "Activated carbon derived from rice husk by NaOH activation and its application in supercapacitor", *Progress in Natural Science: Materials International* **24** (2014) 191–198.
7. A. S. Aricò, P. Bruce, B. Scrosati, J. M. Tarascon, W. Van Schalkwijk. "Nanostructured materials for advanced energy conversion and storage devices", *Nature Materials* **4** (2005) 366 – 377.
8. G. P. Pandey, S. A. Hashmi, Y. Kumar, "Ionic liquid incorporated polymer electrolytes for supercapacitor application", *Indian Journal of Chemistry* **49** (2010) 743-751.
9. V. Khomenko, E. Frackowiak, F. B´eguina, "Determination of the specific capacitance of conducting polymer/nanotubes composite electrodes using different cell configurations", *Electrochimica Acta* **50** (2005) 2499–2506.
10. G. P. Pandey, S. A. Hashmi, Y. Kumar, "Performance Studies of Activated Charcoal Based Electrical Double Layer Capacitors with Ionic Liquid Gel Polymer Electrolytes", *Energy Fuels* **24** (2010) 6644–6652.
11. Cheng-Kim Sim; S.R. Majid, Noor Zalina Mahmood, "Electrochemical Performance of Activated Carbon Derived from Treated Food-Waste", *International Journal of Electrochemical Sciences* **10** (2015) 10157 – 10172.

12. F. Kaasik, T. Tamm, M.M. Hantel, E. Perre, A. Aabloo, E. Lust M.Z. Bazant, V. Presser, "Anisometric charge dependent swelling of porous carbon in an ionic liquid", *Electrochemistry Communications* **34** (2013) 196 – 199.

13. W.J. Cao, J.P. Zheng, "Li-ion capacitors with carbon cathode and hard carbon/stabilized lithium metal powder anode electrodes", *Journal of Power Sources* **213** (2012) 180-185.

14. M.D. Levi, C. Wang, D. Aurbach, "Two parallel diffusion paths model for interpretation of PITT and EIS responses from non-uniform intercalation electrodes", *Journal of Electroanalytical Chemistry* **561** (2004) 1–11.

15. Hainan Wang, Laurent Pilon, "Physical interpretation of cyclic voltammetry for measuring electric double layer capacitances", *Electrochimica Acta* 64 (2012) 130–139.

16. Wen Lu, Kent Henry, Craig Turchi, John Pellegrino, "Ionic Liquid-Incorporated Gel Polymer Electrolytes for Ultracapacitors", *ECS Transactions* **2** (2007) 15-26.

17. R.S. Hastak, P. Sivaraman, D.D. Potphode, K. Shashidhara, A.B. Samui, "All solid supercapacitor based on activated carbon and poly [2,5-benzimidazole] for high temperature application", Electrochimica Acta **59** (2012) 296– 303.

This document was created with the Win2PDF “print to PDF” printer available at
http://www.win2pdf.com

This version of Win2PDF 10 is for evaluation and non-commercial use only.

This page will not be added after purchasing Win2PDF.

http://www.win2pdf.com/purchase/